HOKKAIDO UNIVERSITY

Title	Origin of chiral discrimination by a two-dimensionally chiral self-assembled monolayer : A quantum chemical study
Author(s)	Nishikawa, Tomohiro; Torimoto, Tsukasa; Nakanishi, Takuya; Osaka, Tetsuya; Ohtani, Bunsho
Citation	Chemical Physics Letters, 432(4-6), 502-507 https://doi.org/10.1016/j.cplett.2006.10.106
Issue Date	2006-12-11
Doc URL	http://hdl.handle.net/2115/17175
Type	article (author version)
File Information	CPL432-4-6.pdf

Instructions for use

Origin of chiral discrimination by a two-dimensionally chiral

self-assembled monolayer: A quantum chemical study

Tomohiro Nishikawa [a], Tsukasa Torimoto [b], Takuya Nakanishi [c], Tetsuya Osaka [c], Bunsho

Ohtani [a],*

[a] *Catalysis Research Center, Hokkaido University, Sapporo 001-0021 Japan*

[b] *Graduate School of Engineering, Nagoya University, Furocho, Chikusa-ku, Nagoya*

464-8603 Japan

[c] *School of Science and Engineering, Waseda University, Shinjuku-ku, Tokyo 169-8555 Japan*

Abstract

Structural and energetic investigations based on semiempirical PM5 and ab initio HF and MP2 calculations suggested that the self-assembled monolayer of an atropisomeric compound, (*R*)- or (*S*)-1,1′-binaphthalene-2,2′-dithiol (BNSH), on a gold (111) surface selectively adsorbs one enantiomer of phenylalanine (Phe), resulting in chiral discrimination, through hydrophobic, cation($-NH_3^+$)-π and NH(Phe)-π(BNSH) interactions in a nanometer-sized *screw-hole*-like pocket composed of three BNSH molecules in the monolayer.

* Corresponding author. FAX: +81-11-706-9133.
E-mail address: ohtani@cat.hokudai.ac.jp (B. Ohtani).

1. Introduction

Chiral discrimination, selective interaction of one of the enantiomers of target molecules, is one of the indispensable technological components for fabrication of sensors for chiral molecules, catalysts inducing chiral selective reactions, and chromatography columns for separation of chiral molecules.   One frequently employed technique for chiral recognition is formation of a favored diastereomer composed of the chiral molecule (host) and substrate (guest), which leads to chiral discrimination.

Metal complexes containing an atropisomeric 1,1'-binaphthalene unit as a ligand interact with prochiral substrates to give optically active products [1].   Cyclodextrins and their derivatives have also been used as a chiral host for enantio-selective separation in chromatography [2].   Amphiphilic crown ethers [3] and calixarenes [4,5] in their monolayer on a surface have also been reported to be effective for chiral recognition of amino acids. Another type for chiral recognition on surfaces is adsorption by a crystal surface of chiral atomic arrangements [6,7], though its practical application seems rather limited.

The concept of two-dimensional chirality (TDC) was explored in nanometer scale using a self-assembled monolayer (SAM) of an atropisomeric compound, (*R*)- or (*S*)-1,1′-binaphthalene-2,2′-dithiol (BNSH), on a gold (111) surface, and a stable two-dimensional chiral arrangement of BNSH or its naphthalene moiety, was observed by scanning tunneling microscopy (STM) [8].   The proposed TDC structure, Figs. 1 (a, b), is produced by covalent-bond formation between the sulfur atom in BNSH and the surface gold atom and plausibly by CH-π interaction between adjacent naphthalene groups.   When the (*R*)- or (*S*)-BNSH-modified gold was immersed in aqueous solutions of an enantiomer of either phenylalanine (Phe) [9] or thalidomide [10], the TDC surface adsorbed only one enantiomer of the chiral molecule.

Since the TDC surface is covered with non-polarized naphthalene moieties, it is

thought that hydrophobic interaction occurs between the naphthalene moieties and a hydrophobic part of substrates.   However, the origin of chiral discrimination is still ambiguous at present, since no direct observation of adsorbed species on a TDC surface has yet been successful.   Under these circumstances, the present paper reports on the results of our recent semiempirical and ab initio calculations on the mechanism of this process.

2. Calculation details

2.1. Semiempirical calculation

Calculations concerning a desorption of Phe were performed using the semiempirical PM5 hamiltonian [11] on MOPAC2002 [12,13].   Two model structures of BNSH assembly that have a space large enough to hold a substrate molecule, *screw-hole* (Fig. 1(c)) and *doughnut* (Fig. 1(d)), were chosen assuming host-guest interaction for chiral discrimination. The results of STM analyses have confirmed that *screw-hole* and *doughnut* are composed of three BNSH molecules and six BNSH molecules, respectively [8].   Since both *screw-hole* and *doughnut* share their BNSHs with adjacent units, discussion on their interaction with Phe should be limited only to the configuration where Phe is included in these units.

The model structures were prepared by fixing the positions of sulfur atoms located on the center (three-hold hollow) of three hexagonally-close-packed gold atoms (0.288-nm diameter) [8] and the angles (40.0°) between the carbon-sulfur(I) bond and the gold surface, as shown in Figs. 1(c, d).   The bond lengths between the sulfur atoms are 0.44 and 0.50 nm. The optimization of each geometry was performed using an algorithm of the eigenvector following [14,15].   As shown in Fig. 1(c), the average length of a side of the triangle of the thus-optimized *screw-hole* structure was 1.56 nm, which agreed well with the experimental value of 1.62 nm [8].   Phe, a zwitter-ionic chiral amino acid, was used as an analyte molecule for comparison with the experimental results.   The *screw-hole* has a dimple with the maximum width of 1.20 nm and the depth of 0.60 nm, and *doughnut* has a large enough

cavity (the opening width of 0.80 nm and the depth of 0.60 nm) to hold substrate molecules. The initial geometries of Phe in chiral substrates, shown in Fig. 2(a), were settled by facing its phenyl group toward the bottom of *screw-hole*s and *doughnut*s, because no local minima were obtained when the amino and carboxyl groups of Phe were set upside-down in the inside of *screw-hole*s and *doughnut*s.   The initial geometry of Phe was set on an anchoring point, A_p in Fig. 2(b), and the reaction coordinate h is defined as the distance between A_p and the nearest neighboring phenyl carbon atom (C_1) to the bottom of the chiral units A_p in Fig. 2(c).   The potential energy curves for the Phe desorption from *screw-hole* and *doughnut* were determined by calculating the change in the heat of formation for the optimized geometry of Phe at each distance from the anchoring point of *screw-hole* or *doughnut*.

2.2. Ab initio calculations

Ab initio calculations were performed using Gaussian 03 [16].   All geometries of single point calculations were based on the structures of PM5 optimization.   The adsorption energies of Phe were estimated by subtracting the energies of the stable complex from the sum of energies of each isolated component, i.e., by the supermolecule method.   The calculations of the adsorption energies for the four local-minimum states employing the whole model of *screw-hole* were carried out using HF/6-31G**.   For two representative states, adsorption energies corrected for the basis-set superposition error (BSSE) by the counterpoise method [17,18] were calculated by the model in which *screw-hole* was separated into three BNSH parts using MP2/6-311G**.   The MP2 adsorption energies are estimated as the sum of three interaction energies between each BNSH part and Phe.

3. Results and discussion

3.1. Semiempirical calculation on the desorption of Phe from screw-holes and doughnuts

The potential curves for desorption of D- and L-Phe from chiral units are shown in Fig. 3.   The curves for (*R*)- and (*S*)-*screw-hole*s are of similar shape until the desorption point at

which C_1 carbon of Phe is located above the hypothetical plane including the tops of BNSHs, as indicated by arrows in Figs. 3(a) and (b). It seems reasonable to see nearly identical curves for each enantiomeric pair of complexes, (*R*)-L and (*S*)-D, as well as (*R*)-D and (*S*)-L. These curves give a local minimum at 0.36-0.38 nm and tend to a plateau at 0.60-0.80 nm. Discontinuities after this plateau are attributed to irregular interactions with the outside wall of the unit, which is not expected in the actual TDC structure. The changes in the heat of formations are presented by adjusting the energy of the desorbed point to be zero for clarity. The absolute values of the heat of formation at the minimum points are nearly equal, within 2 kJ mol^{-1}, for all the combinations. Therefore, we do not discuss the difference due to chirality here, but an appearance of this energy minimum in each curve suggests that Phe can be adsorbed by the nanostructure.

On the other hand, *doughnut*s also give a local minimum in the potential curves, as shown in Figs. 3(c) and (d), but the potential dips seem to be shallower than *screw-hole*s. The adsorption energy calculated by the supermolecule method for *doughnut*s is 40 kJ mol^{-1} smaller than that of *screw-hole*s. Thus, we conclude that *screw-hole*, but not *doughnut*, is responsible for the chiral recognition by TDC.

3.2. Ab initio calculation of adsorption energies

The results of ab initio calculations for the adsorption energy are listed in Table 1. The adsorption energies for (*R*)-L and (*S*)-D complexes by HF/6-31G** are larger than those for (*R*)-D and (*S*)-L, which agree well with the experimental results [9]. Also, the order of BSSE-corrected HF energies for (*R*)-D and (*R*)-L complexes is unchanged. We note in this connection that a significant contribution of dispersion force was indicated in the electron-correlation calculations of the interaction between the aromatic rings of BNSH and Phe by MP2 [19,20], where the BSSE-corrected MP2 interaction energies were estimated to be larger than those with HF. The difference in the adsorption energy by MP2, ~ 27 kJ mol^{-1},

seems to induce chiral discrimination.   Assuming a simple relation between the adsorption equilibrium constant K at 298 K and the Gibbs energy of adsorption, $\Delta G = -RT \ln K$ and approximating ΔG by the adsorption energy estimated above, the equilibrium constants for the favorable combinations are estimated to be $\sim 6 \times 10^4$ times larger than those of other unfavorable combinations.

3.3. Interaction with naphthalene moieties and amino group

As shown in Table 2, the interaction energies of Phe for BNSH-2 and BNSH-3 are 50-70 kJ mol^{-1}.   These energies corresponded to the interaction between the naphthalene moieties in BNSHs and the phenyl group of Phe.   On the other hand, the interaction energy between BNSH-1 and Phe is somewhat larger, ~ 150 kJ mol^{-1}, presumably due to the additional interaction between the amino group of Phe and naphthalene moieties in BNSHs. The amine-aromatic interaction as indicated by the difference, 80-100 kJ mol^{-1}, is attributable to cation($-NH_3^+$)-π interaction; similar energy has been reported for Na$^+$-π interaction [21]. A relatively small difference in the partial adsorption energy of BNSH-1 with D- and L-Phe suggests that such cation-π interaction stabilizes the adsorption but that BNSH-1 part hardly induces chiral discrimination.

Several reports have been made on another type of interaction of an amino group with aromatic rings.   For example, Rodham et al. made a report based on their spectroscopic measurements and ab initio calculations that an amine is located on a benzene plane by a hydrogen bonding between the N-H bond and the π-electron cloud [22].   Tsuzuki et al. studied the orientation of ammonia facing a benzene plane using high-level ab initio calculations and suggested that an intermolecular NH-π interaction is induced between the N-H bond and a π-electron molecule [23].   On the basis of these considerations, we infer that the chiral discrimination by TDC is regulated by the NH-π interaction, as described in the following section.

6

3.4. Structure of the complexes between screw-holes and Phe

The structure of stable complexes including (*R*)-*screw-hole* is shown in Fig. 4. The structure of (*S*)-*screw-hole* is of mirror image. The phenyl group in D- or L-Phe is located at almost the center in *screw-hole* with an average distance of 0.49 nm between the carbon atoms of three naphthalene moieties in *screw-hole* and C_1 in the phenyl group of Phe. The closest distance, 0.29 nm, between *screw-hole* and Phe is observed at an amino group facing a naphthalene moiety. Resonance and exchange energies are not expected for any atoms between *screw-hole* and Phe, and no chemical bonds were observed between Phe and BNSHs. In other words, these features suggest that the phenyl group in Phe is floating, without face-to-face π-π stacking, in *screw-hole* owing to the hydrophobic interaction between Phe and three BNSHs in *screw-hole* and that the amino group interacts with the upper part of the naphthalene moiety of BNSH. One possible reason for this floating is the twisted arrangement of naphthalenes prohibiting face-to-face stacking of the phenyl groups due to their steric hindrance.

The difference between the Phe isomers, which influences the stability of complexes, is the direction of a carbon-amino (ammonium) nitrogen bond against the neighboring naphthalene moiety. In the favorable arrangement with L-Phe, all three N-H bonds in the ammonium group are facing the neighboring naphthalene with nearly equal distances, whereas no such confrontation can be achieved in unfavorable arrangements (Fig. 4). Since the observed distances between the nitrogen atom and naphthalene are nearly equal, 0.29 nm, one can assume that the cation-π interactions between the isomers are essentially identical. Therefore, the arrangement of Phe in *screw-hole* may be understood as regulated by the NH-π interaction, though the reported energy [23], is as small as ~8 kJ mol^{-1} (24 kJ mol^{-1} for three N-Hs). As shown in Table 2, the difference in the adsorption energy between D- and L-Phe is mainly due to those in the interaction with BNSH-2 and BNSH-3, i.e., the adsorption-energy

difference is probably caused by the enhanced interaction between Phe and BNSH-2/BNSH-3 owing to the preferred arrangement of Phe regulated by the NH-π interaction.

3.5. Characteristics of chiral discrimination by TDC-SAM

The mechanisms of chiral discrimination proposed earlier, within our knowledge, included chemical bond(s) with functional groups, e.g., the guanidinium moiety [4] and the carboxyl and amino groups in Phe [5].   However, the present chiral recognition with TDC appears to be different from the conventional cases, especially in the following three points: (1) No chemical bonds seem to be involved; i.e., Phe is captured only by hydrophobic, cation-π and NH-π interactions.   (2) The discrimination is caused by the twisted morphology of D- and L-Phe.   We note that TDC consists of naphthalene groups only, with no other functional groups.   (3) The carboxylate group in Phe does not participate in the interaction of TDC and Phe.   As far as we know, most part of the reported chiral discrimination of amino acids, e.g., chiral separation in chiral HPLC columns, has been achieved using chelation of metal ions with their amino and carboxyl groups, and therefore, the present system can be categorized into a *novel* type of chiral discrimination.   These features strongly suggest that TDC could discriminate chirality of a wide range of chiral aromatic compounds having twisted morphologies, not only amino acids containing a phenyl group.   In fact, TDC also discriminates chirality of thalidomide almost perfectly [10].   A preliminary quantum chemical calculation of the interaction of thalidomide with TDC has also achieved reproduction of chiral discrimination with *screw-hole*s.

4. Conclusions

Quantum chemical calculations on the structure and adsorption energy of TDC with Phe have indicated that TDC discriminates chirality of Phe in a "screw-screw hole" fashion that is different from conventional mechanisms.   This behavior appears to be flexible toward a wide range of chiral substrates.   The present finding suggests that quantum chemical

calculation is applicable for a survey of chiral compounds separable by TDC and for a more accurate analysis of molecular interactions affecting the complexation and chiral discrimination by TDC-SAM.

References

[1]   R. Noyori, Angew. Chem. Int. Ed. 41 (2002) 2008.

[2]   B. Chankvetadze, Chem. Soc. Rev. 33 (2004) 337.

[3]   M. Badis, I. Tomaszkiewicz, J.-P. Joly, E. Rogalska, Langmuir 20 (2004) 6259.

[4]   F. Liu, G.-Y. Lu, W.-J. He, M.-H. Liu, L.-G. Zhu, Thin Solid Films 468 (2004) 244.

[5]   P. Shahgaldian, U. Pieles, M. Hegner, Langmuir 21 (2005) 6503.

[6]   A. Ahmadi, G. Attard, J. Feliu, A. Rodes, Langmuir 15 (1999) 2420.

[7]   O.A. Hazzazi, G.A. Attard, P.B. Wells, J. Mol. Catal. A: Chem. 216 (2004) 247.

[8]   B. Ohtani, A. Shintani, K. Uosaki, J. Am. Chem. Soc. 121 (1999) 6515.

[9]   T. Nakanishi, N. Yamakawa, T. Asahi, T. Osaka, B. Ohtani, K. Uosaki, J. Am. Chem. Soc. 124 (2002) 740.

[10] T. Nakanishi, N. Yamakawa, T. Asahi, N. Shibata, B. Ohtani, T. Osaka, Chirality 16 (2004) S36.

[11] "MOPAC2002", Fujitsu Limited, Tokyo, 2004.

[12] J.J.P. Stewart, MOPAC: A General Molecular Orbital Package, Quant. Chem. Prog. Exch. 10 (1990) 86.

[13] "MOPAC2002", J.J.P. Stewart, Fujitsu Limited, Tokyo, 2001.

[14] A. Banerjee, N. Adams, J. Simons, R. Shepard, J. Phys. Chem. 89 (1985) 52.

[15] P. Culot, G. Dive, V.H. Nguyen, J.M. Ghuysen, Theo. Chim. Acta. 82 (1992) 189.

[16] "Gaussian 03, Revision C.02", M. J. Frisch et al., Gaussian, Inc., Wallingford, CT, 2004.

[17] B. Ransil, J. Chem. Phys. 34 (1961) 2109.

[18] S.F. Boys, F. Bernardi, Mol. Phys. 19 (1970) 553.

[19] S. Tsuzuki, K. Honda, T. Uchimaru, M. Mikami, K. Tanabe, J. Am. Chem. Soc. 124 (2002) 104.

[20] S. Tsuzuki, K. Honda, T. Uchimaru, M. Mikami, J. Chem. Phys. 120 (2004) 647.

[21] S. Tsuzuki, T. Uchimaru, M. Mikami, J. Phys. Chem. A 105 (2001) 769.

[22] D.A. Rodham, S. Suzuki, R.D. Suenram, F.J. Lovas, S. Dasgupta, W.A. Goddard III, G.A. Blake, Nature 362 (1993) 735.

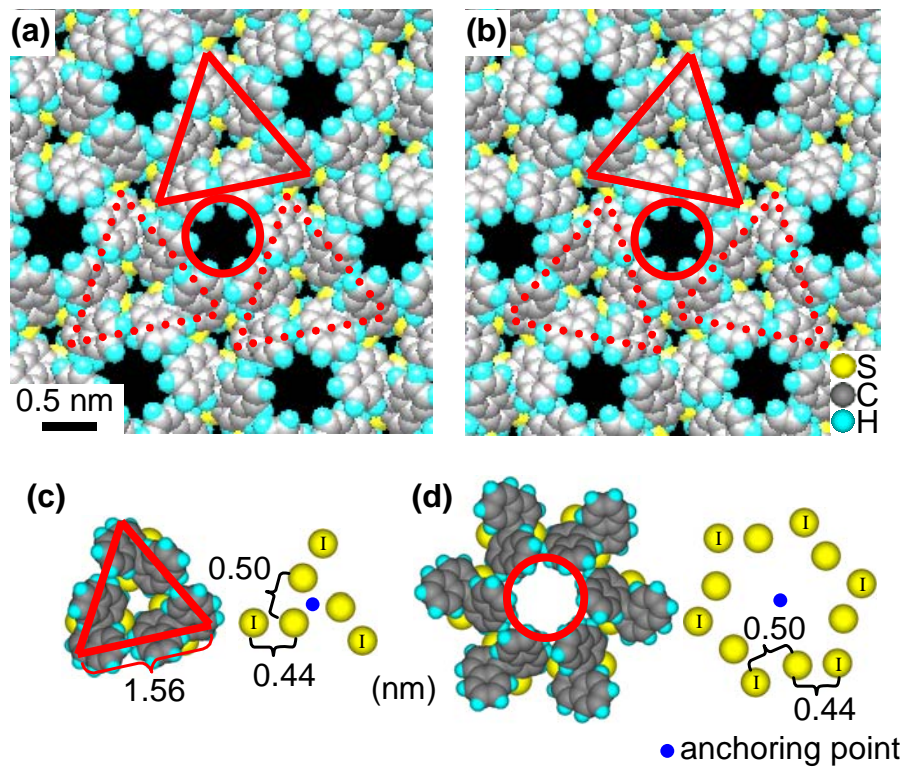[23] S. Tsuzuki, K. Honda, T. Uchimaru, M. Mikami, K. Tanabe, J. Am. Chem. Soc. 122 (2000) 11450.

Fig. 1 Two-dimensional chirality of (*R*)-TDC (a), (*S*)-TDC (b) and a calculation model of (*R*)-*screw-hole* (c) and (*R*)-*doughnut* (d). Points shown in blue in (c) and (d) are hypothetical anchoring points, A_p; see text.
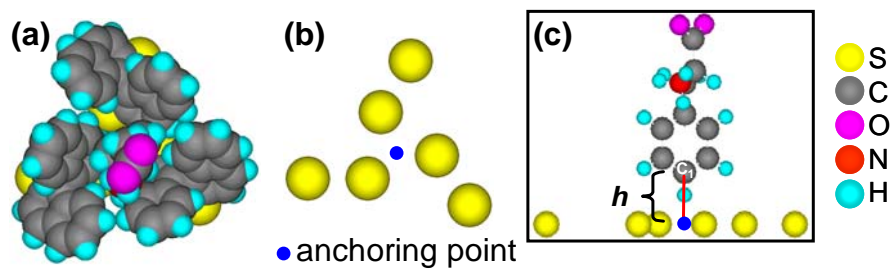
Fig. 2 Initial geometry of phenylalanine in *screw-hole* (a) and definition of the reaction coordinate of phenylalanine desorption calculation (b, c).
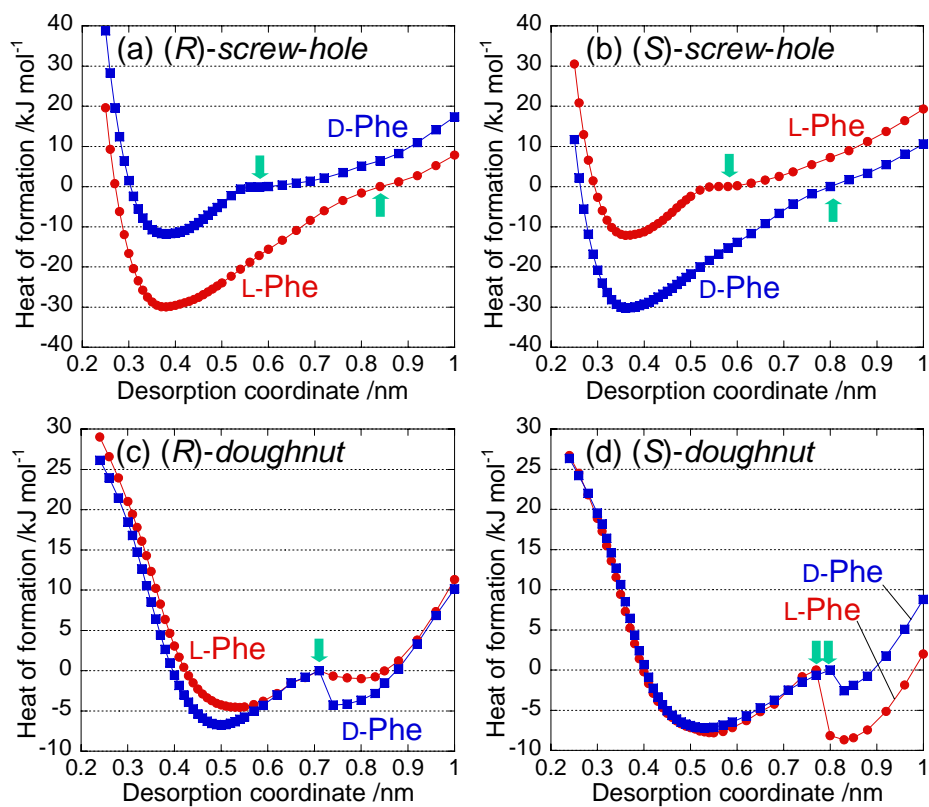
Fig. 3 Potential curves for the desorption of Phe from *screw-hole* and *doughnut* using semi-empirical PM5 calculation. Arrows indicate points of desorption.
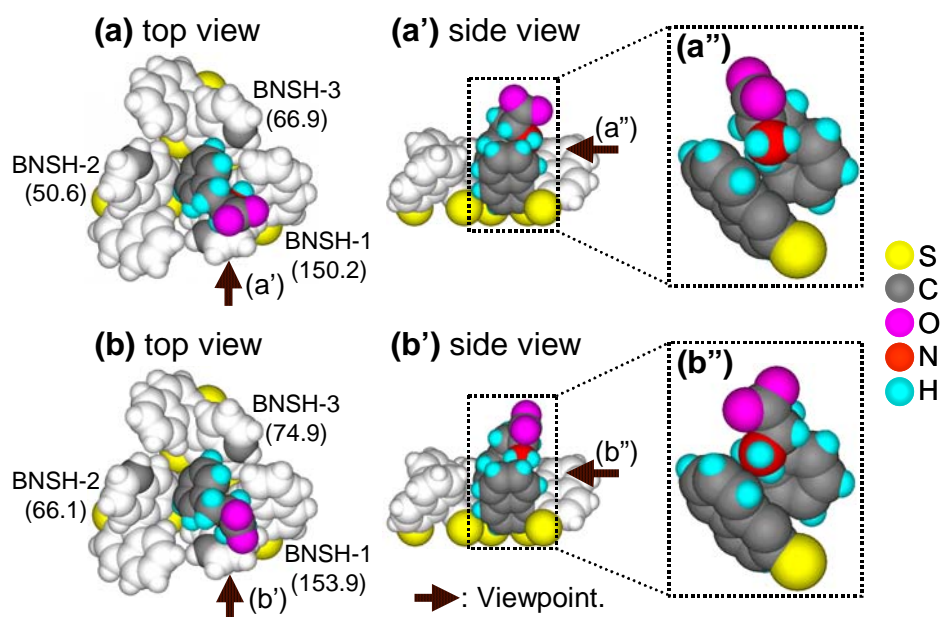
Fig. 4 Proposed most stable structures of adsorption of D-Phe (a) and L-Phe (b) in (*R*)-*screw-hole*. Numbers in parentheses are MP2 interaction energies in kJ mol^{-1}. See Table 2.

Table 1
Energies of adsorption [a] of D- and L-phenylalanine in *screw-hole*s (in kJ mol^{-1})

	HF/6-31G**		HF/6-311G**		MP2/6-311G**	
	D-Phe	L-Phe	D-Phe	L-Phe	D-Phe	L-Phe
(*R*)-*screw-hole*	142.8	239.3	83.0	186.3	267.8	294.9
(*S*)-*screw-hole*	229.5	127.7				

[a] BSSE-correction is included except in HF/6-31G** calculations.

Table 2
Separated BSSE-corrected interaction energies of D- and L-phenylalanine for each part of (*R*)-*screw-hole* (in kJ mol^{-1})

	MP2/6-311G**		
	BNSH-1	BNSH-2	BNSH-3
D-phenylalanine	150.2	50.6	66.9
L-phenylalanine	153.9	66.1	74.9